Recent Advances in Fabricating Wurtzite AlN

Subjects: Materials Science, Coatings & Films | Crystallography | Materials Science, Composites
Contributor: Chenguang He

As a representative ultrawide bandgap (UWBG) semiconductor material, wurtzite aluminum nitride (AlN) material has many excellent properties such as high electron mobility (1100 cm2/Vs), high breakdown voltage (11.7 MV/cm), high piezoelectric coefficient, high thermal conductivity (320 W/m·K), high hardness (nine on the Mohs scale), high corrosion resistance, high chemical and thermal stability, as well as high bulk acoustic wave velocity (11,270 m/s).

AlN | sapphire | Heteroepitaxy | MOCVD | Crystal Growth | Dislocation | Strain | Thermal Conductivity | Polarity Control

1. Introduction

AlN crystal has three possible structures: hexagonal wurtzite structure, cubic zinc blende structure, and rock salt structure [1]. Among them, metastable-phase cubic zinc blende structure and rock salt structure only exist in some special growth conditions. In most cases, the hexagonal wurtzite structure is needed because its excellent chemical stability is helpful to obtain highly reliable devices. However, the high chemical stability makes it quite challenging to grow high-crystalline-quality bulk AlN crystals. Growing bulk crystals from the melt, which is performed for most other III–V semiconductors, is no longer applicable to AlN because ultrahigh temperature and pressure are needed. Nowadays, bulk AlN crystals are nearly exclusively obtained by using the physical vapor transport (PVT) method (sublimation and recondensation), which has achieved low TDDs of 10^2–10^5 cm^{-2} [2]. Nevertheless, it still cannot solve the typical problems such as small size (<60 mm), high impurity concentration (10^{18}–10^{19} cm^{-3}), poor ultraviolet transparency ($\alpha_{265–280\ nm}$ = 14–21 cm^{-1}), and high cost (>9000 USD/2 inch) [3]. Only a few companies can supply bulk AlN in the world, and the production capacity is very low due to the very long growth time and very low yield. As an alternative, depositing thin AlN films on foreign substrates such as sapphire, silicon (Si), and silicon carbide (SiC) has become the prevailing method to obtain AlN crystals [4][5][6]. These pseudo-substrates are also called AlN templates. Among them, the most commonly used foreign substrate is sapphire, which is commercially available in various sizes (2–8 inches) and surface orientations (*c*, *m*, *r*, and *a* planes). Importantly, the crystalline quality of AlN/sapphire template is relatively good, and the cost of AlN/sapphire template has been reduced to 250 USD/2 inch. The deposition methods include metal organic chemical vapor deposition (MOCVD), molecular beam epitaxy (MBE), hydride vapor phase deposition (HVPE), physical vapor deposition (PVD), pulsed laser deposition (PLD), and atomic layer deposition (ALD).

2. Polarity Control of AlN/Sapphire Template

The polarity control is very important for AlN-based devices, because polarity greatly affects the electronic and optoelectronic properties by changing the pyroelectric and piezoelectric fields [7]. The polarities of AlN include Al-polarity (+*c*-polarity) and N-polarity (−*c*-polarity). Except for some special applications such as lateral polarity structure (LPS) and N-polar high electron mobility transistors (HEMTs) [8][9], N-polar AlN is not desired because of its poor crystalline quality, surface morphology, and chemical stability. Ronny Kirste et al. demonstrated the surface of N-polar AlN was dominated by a typical columnar morphology, with an average width of ~500 nm and a height difference of ~100 nm [10], as shown in **Figure 1**. The rough surface morphology originated from the presence of Al-polar inversion domains (IDs), which had a faster growth rate along the [0001] direction. Other studies have also confirmed that N-polar AlN usually coexists with Al-polar AlN IDs, meaning that AlN film grown on sapphire substrate generally exists in two forms: Al-polar AlN and mixed-polar AlN. To realize large-area pure N-polar AlN, C-face SiC substrate may be the better choice [11]. The mixed-polar AlN can be confirmed by the KOH solution etching because N-polar AlN has an obvious faster etching rate compared with Al-polar AlN. **Figure 2** displays some etched surfaces of AlN epilayers grown in different conditions [12]. The etched parts are N-polar AlN, and the residual parts are Al-polar AlN.

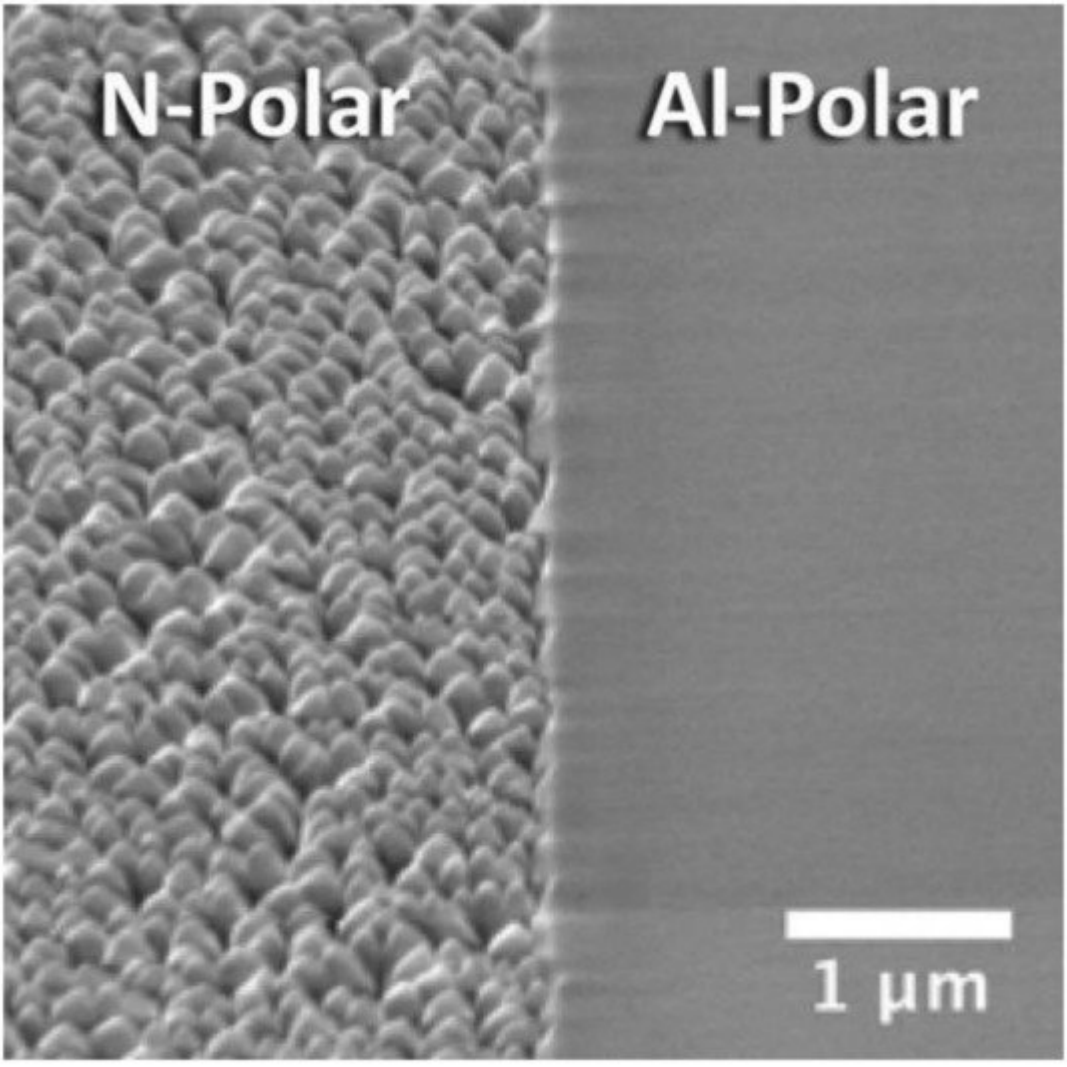

Figure 1. Morphology difference between N-polar and Al-polar AlN on the same wafer. Reprinted from [10], with the permission of AIP Publishing.

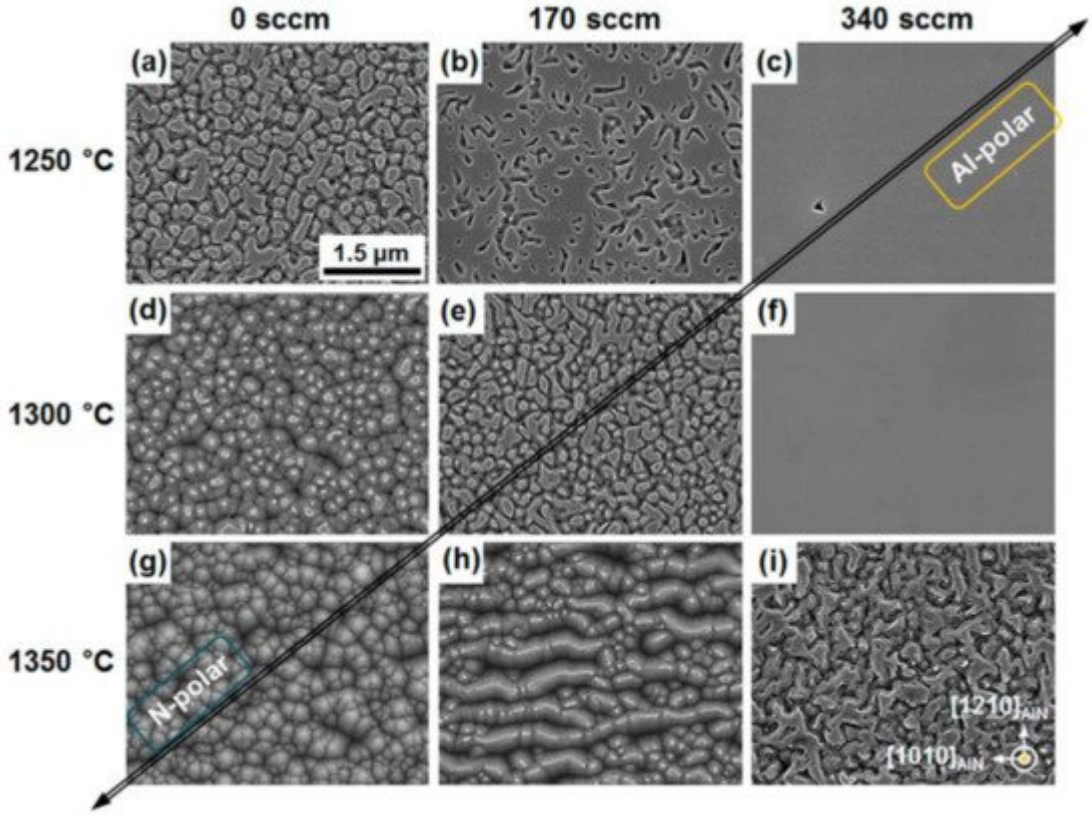

Figure 2. (**a**–**i**) Plan-view scanning electron microscope (SEM) images of KOH-etched AlN/sapphire templates, which were grown on different conditions (Temperatures = 1250, 1300, and 1350 °C; TMAl flows = 0, 170, and 340 sccm). Reprinted with permission from [12]. Copyright {2015} American Chemical Society.

Compared with other nitride semiconductors, the polarity control of AlN film grown on sapphire substrate is much more difficult. It is attributed to the formation of unevenly distributed aluminum-oxynitride ($Al_xO_yN_z$) phases near the AlN/sapphire interface, which is responsible for the appearance of mixed-polar AlN. $Al_xO_yN_z$ phases can exist with various stoichiometric ratios, depending on the competition result of Al, O, and N atoms [13]. Since the 1970s, various $Al_xO_yN_z$ phases have been established, including 20*H* ($Al_{10}O_3N_8$), 27*R* ($Al_9O_3N_7$), 16*H* ($Al_8O_3N_6$), 21*R* ($Al_7O_3N_5$), 12*H* ($Al_6O_3N_4$), and many other phases [14]. These O atoms may come from sapphire substrate, precursors and chambers, so they are hard to completely eliminate. To suppress the undesired N-polar AlN/mixed-polar AlN, we need to find out the key factors affecting polarity control in the presence of O atoms.

H. D. Sun et al. found that proper TMAl pretreatment promoted the formation of Al-polar AlN, because carbon (C) impurities dissociated from TMAl precursor could attract surrounding O impurities and suppress the formation of $Al_xO_yN_z$ phases [15]. Cross-sectional energy-loss spectroscopy spectrum (EELS) demonstrated that the distributions of C and O atoms above the AlN/sapphire interface are highly consistent. J. M. Wang et al. found that 7 s NH_3 preflow (nitridation) could also maintain Al-polar AlN, and the *c*-axis orientation was very good [16]. However, a longer-time NH_3 preflow resulted in the formation of mixed-polar AlN. Obviously, the pretreatment

process before the deposition of AlN film is very important. Additionally, it was found that high initial growth temperature facilitates the formation of N-polar AlN. Reina Miyagawa et al. revealed that a certain chemical reaction occurred during the high-temperature growth process, causing the exchange of O atoms in sapphire substrate and N atoms in AlN epilayer in some areas [17]. As a result, Al-polar and N-polar AlN simultaneously appeared and coexisted in the subsequent growth process, because the large N-polar AlN grains at high growth temperature were hard to bury.

In some special cases, the transition from pure N-polar or mixed-polar AlN to pure Al-polar AlN may occur. Stefan Mohn et al. demonstrated that pure N-polar AlN could be entirely converted into Al-polar AlN within 3 nm, with the help of a flat rhombohedral $Al_xO_yN_z$ layer [18]. Scanning transmission electron microscope (STEM) and high-resolution transmission electron microscopy (HRTEM) images revealed that the conversion had been completed during the nitridation process before growth, as shown in **Figure 3**. However, excessive annealing may destroy the $Al_xO_yN_z$ structure, leading to incomplete coverage of the $Al_xO_yN_z$ layer, especially when the annealing temperature is very high. In this situation, the undesirable mixed-polar AlN is formed due to the incomplete conversion of N-polar AlN to Al-polar AlN. Mitsuru Funato et al. reported that N-polar AlN domains in mixed-polar AlN could be buried by their surrounding Al-polar AlN, as shown in **Figure 4**. This phenomenon occurred when the nitridation of sapphire substrate initiated at a low temperature of 100 °C [19]. The elimination of N-polar AlN domains benefited from the small size of inversion domains and the faster growth rate of Al-polar AlN [12]. Based on the above analysis, we can see that the realization of pure Al-polar AlN has three approaches: suppressing the local formation of $Al_xO_yN_z$ phases in the initial stage, converting N-polar to Al-polar AlN by the complete coverage of ultrathin $Al_xO_yN_z$ layer, and burying N-polar AlN by the lateral overgrowth of Al-polar AlN.

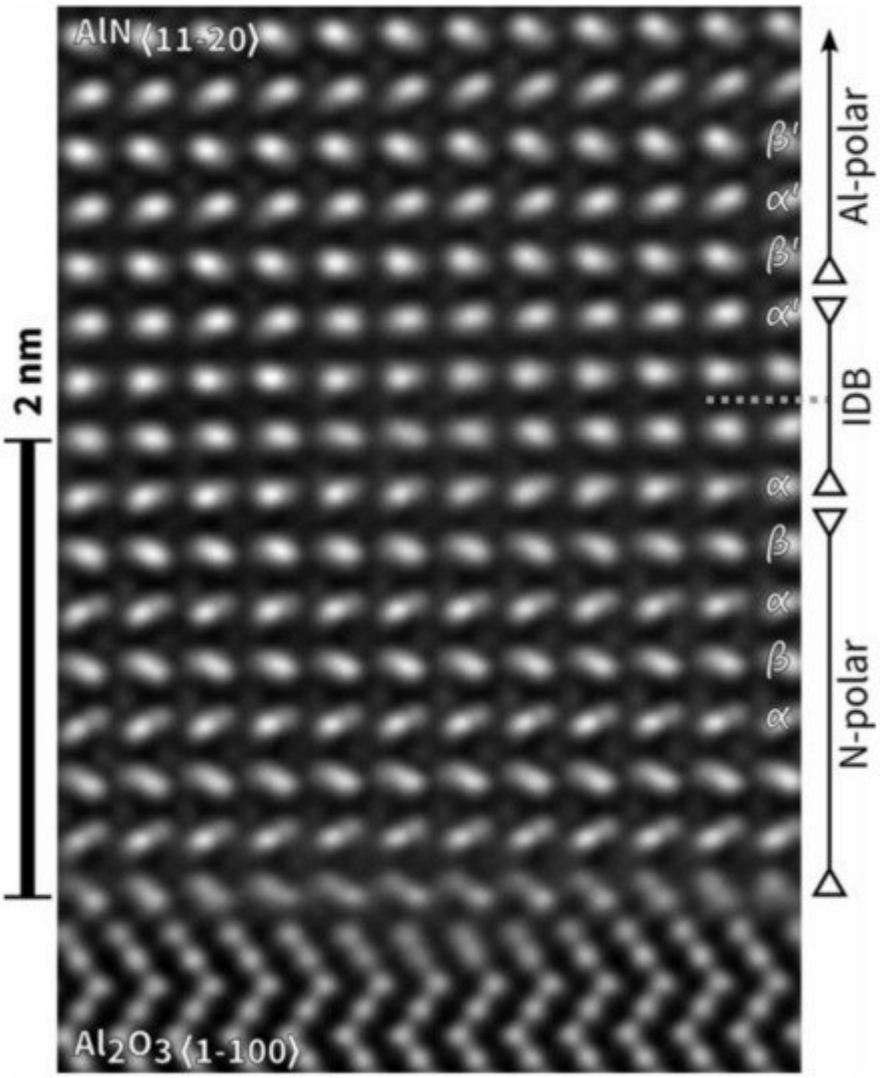

Figure 3. Cross-sectional HRTEM image of AlN/sapphire template. The polarity of AlN epilayer evolved from N-polar to Al-polar within 3 nm above the AlN/sapphire interface. Reprinted from [18] under the terms of the Creative Commons Attribution 3.0 License.

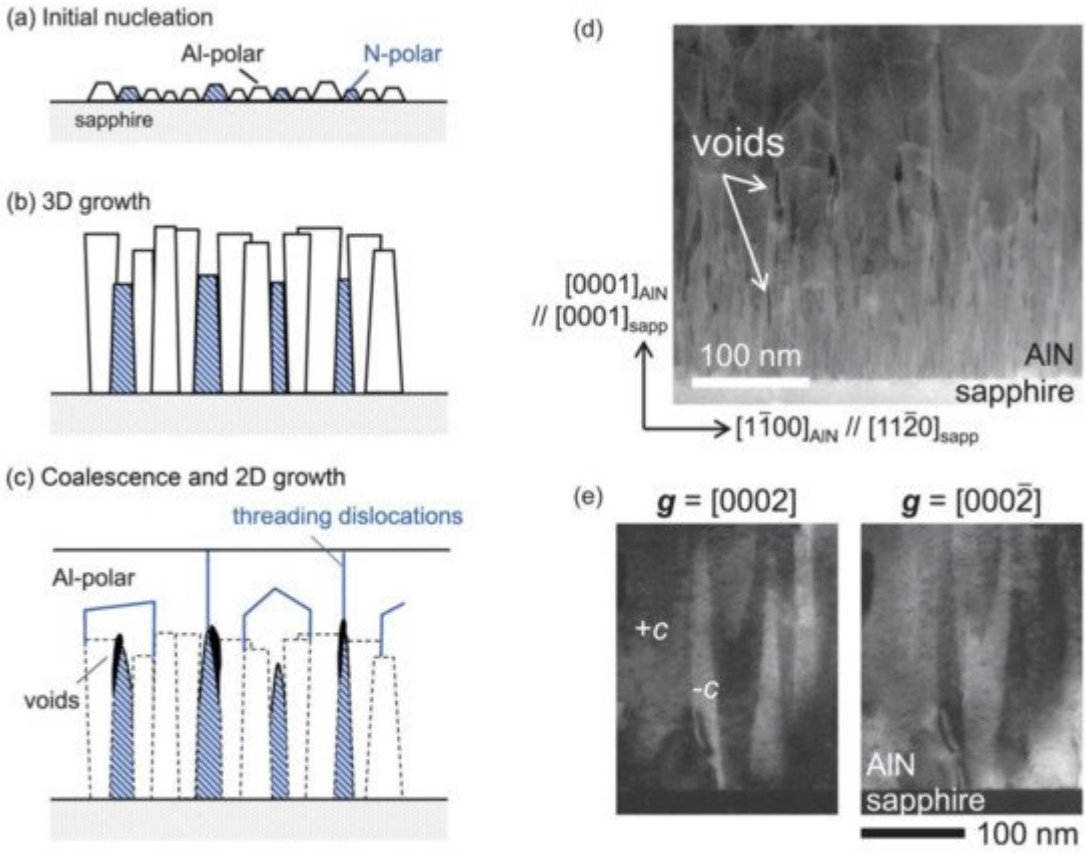

Figure 4. Schematic diagrams of the lateral burying process of N-polar AlN by Al-polar AlN: (**a**) the initial nucleation stage; (**b**) 3D growth stage; (**c**) coalescence and 2D growth stage; (**d**) cross-sectional TEM image of the lateral burying process of N-polar AlN by Al-polar AlN. Lots of voids formed above the N-polar AlN after the entire burying of N-polar AlN; (**e**) cross-sectional TEM dark field (DF) images taken at the same position using two-beam conditions. Lots of columnar structures with a width of tens of nanometers can be observed, indicating the co-existence of Al-polar AlN and N-polar AlN. Reprinted from [19], with the permission of AIP Publishing.

3. The TDD Compilation of AlN Films Grown by Different Techniques

Figure 5 summarizes the reported TDD values (2005–2021) of AlN films grown by different techniques. The laboratory level of TDD can be decreased to <5 × 10^7 cm^{-2} by using ELOG, HTA, and MSG growth techniques, and the industrialization level of TDD is decreased to 10^8–10^9 cm^{-2}.

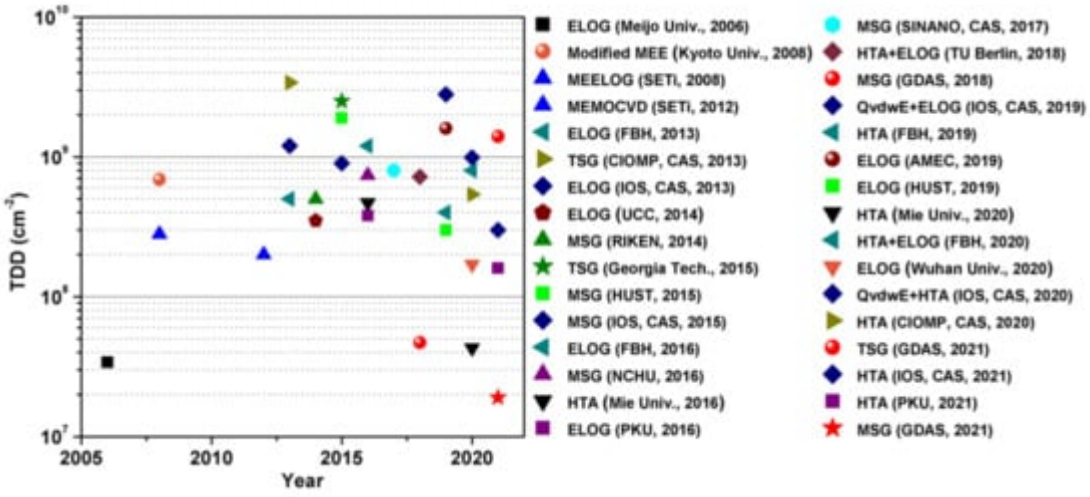

Figure 5. Selected AlN/sapphire TDD by year of publication [4][20][21][22][23][24][25][26][27][28][29][30][31][32][33][34][35][36][37][38][39][40][41][42][43][44][45][46][47][48][49]. The ultralow TDD value of 3.4 × 10^7 cm^{-2} has been achieved by ELOG growth technique in 2006. Since 2018, MSG and HTA growth techniques have also achieved ultralow TDD values below 5 × 10^7 cm^{-2}.

It is noted that there has been no unified standard for the evaluation of TDD. X-ray rocking curve (XRC) scan is the most common method to evaluate TDD. However, X-ray has a large penetration depth in AlN material, meaning that the measurement result containing the information of the whole AlN epilayer rather than that of the top AlN epilayer [50]. Thus, the TDD of the top AlN epilayer extracted from XRC scan is usually overestimated, especially when the TDD is low. Cross-sectional TEM and plan-view TEM results can give the TDD of the top AlN layer, as shown in **Figure 6**. Nevertheless, they have certain degrees of randomness, since the measurement area is usually <50 μm^2 [4][25][33]. Plan-view cathodoluminescence (CL) spectroscopy, which is frequently used to count the TDD of GaN epilayer, is no longer applicable to AlN because of the poor conductivity of AlN and the weak responsivity of the detector at ~200 nm. The TDD evaluated by etch pit density is also inaccurate when the AlN surface is under etched or over etched [51]. Additionally, even if the measurement method is the same, different equipment may obtain different results. Therefore, strictly speaking, the TDD results from different groups or evaluated by different methods should not be directly compared. Here, we list some representative TDD values to see the general development trend.

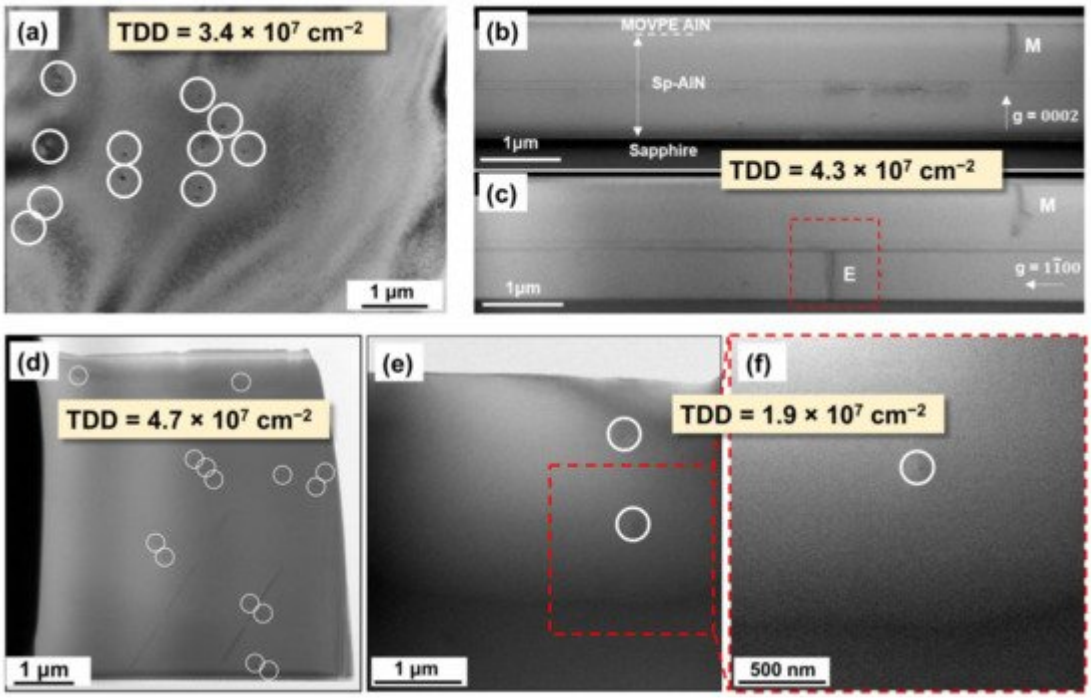

Figure 6. (**a**) Plan-view TEM image of ELOG-AlN grown by Meijo University. Reprinted from J. Cryst. Growth, 298, Masataka Imura et al., "Epitaxial lateral overgrowth of AlN on trench-patterned AlN layers", 257–260, Copyright (2007), with permission from Elsevier. (**b**,**c**) Cross-sectional TEM images of HTA-AlN grown by Mie University. Reprinted from [33]. Copyright (2020) The Japan Society of Applied Physics. (**d**) Plan-view TEM image of 5.6 μm-thick MSG-AlN grown by Guangdong Academy of Sciences (GDAS). Reprinted with permission from [4]. Copyright {2018} American Chemical Society. (**e**,**f**) Plan-view TEM images of 11 μm-thick MSG-AlN grown by GDAS.

References

1. Li, D.; Jiang, K.; Sun, X.; Guo, C. AlGaN photonics: Recent advances in materials and ultraviolet devices. Adv. Opt. Photonics 2018, 10, 43–110.
2. Yu, R.; Liu, G.; Wang, G.; Chen, C.; Xu, M.; Zhou, H.; Wang, T.; Yu, J.; Zhao, G.; Zhang, L. Ultrawide-bandgap semiconductor AlN crystals: Growth and applications. J. Mater. Chem. C 2021, 9, 1852–1873.
3. Wang, Q.; Lei, D.; He, G.; Gong, J.; Huang, J.; Wu, J. Characterization of 60 mm AlN Single Crystal Wafers Grown by the Physical Vapor Transport Method. Phys. Status Solidi A 2019, 216, 1900118.
4. He, C.; Zhao, W.; Wu, H.; Zhang, S.; Zhang, K.; He, L.; Liu, N.; Chen, Z.; Shen, B. High-quality AlN film grown on sputtered AlN/sapphire via growth-mode modification. Cryst. Growth Des. 2018, 18, 6816–6823.
5. Shen, J.; Yang, X.; Liu, D.; Cai, Z.; Wei, L.; Xie, N.; Xu, F.; Tang, N.; Wang, X.; Ge, W. High quality AlN film grown on a nano-concave-circle patterned Si substrate with an AlN seed layer. Appl.

Phys. Lett. 2020, 117, 22103.

6. Zollner, C.J.; Almogbel, A.; Yao, Y.; SaifAddin, B.K.; Wu, F.; Iza, M.; DenBaars, S.P.; Speck, J.S.; Nakamura, S. Reduced dislocation density and residual tension in AlN grown on SiC by metalorganic chemical vapor deposition. Appl. Phys. Lett. 2019, 115, 161101.
7. Ambacher, O.; Smart, J.; Shealy, J.; Weimann, N.; Chu, K.; Murphy, M.; Schaff, W.; Eastman, L.; Dimitrov, R.; Wittmer, L. Two-dimensional electron gases induced by spontaneous and piezoelectric polarization charges in N-and Ga-face AlGaN/GaN heterostructures. J. Appl. Phys. 1999, 85, 3222–3233.
8. Guo, W.; Sun, H.; Torre, B.; Li, J.; Sheikhi, M.; Jiang, J.; Li, H.; Guo, S.; Li, K.H.; Lin, R. Lateral-polarity structure of AlGaN quantum wells: A promising approach to enhancing the ultraviolet luminescence. Adv. Funct. Mater. 2018, 28, 1802395.
9. Ito, T.; Sakamoto, R.; Isono, T.; Yao, Y.; Ishikawa, Y.; Okada, N.; Tadatomo, K. Growth and Characterization of Nitrogen-Polar AlGaN/AlN Heterostructure for High-Electron-Mobility Transistor. Phys. Status Solidi. B 2020, 257, 1900589.
10. Kirste, R.; Mita, S.; Hussey, L.; Hoffmann, M.P.; Guo, W.; Bryan, I.; Bryan, Z.; Tweedie, J.; Xie, J.; Gerhold, M. Polarity control and growth of lateral polarity structures in AlN. Appl. Phys. Lett. 2013, 102, 181913.
11. Lemettinen, J.; Okumura, H.; Kim, I.; Rudzinski, M.; Grzonka, J.; Palacios, T.; Suihkonen, S. MOVPE growth of nitrogen-and aluminum-polar AlN on 4H-SiC. J. Cryst. Growth 2018, 487, 50–56.
12. Eom, D.; Kim, J.; Lee, K.; Jeon, M.; Heo, C.; Pyeon, J.; Nam, O. AlN nanostructures fabricated on a vicinal sapphire (0001) substrate. Cryst. Growth Des. 2015, 15, 1242–1248.
13. Akiyama, T.; Saito, Y.; Nakamura, K.; Ito, T. Nitridation of Al2O3 surfaces: Chemical and structural change triggered by oxygen desorption. Phys. Rev. Lett. 2013, 110, 26101.
14. McCauley, J.W.; Patel, P.; Chen, M.; Gilde, G.; Strassburger, E.; Paliwal, B.; Ramesh, K.; Dandekar, D.P. AlON: A brief history of its emergence and evolution. J. Eur. Ceram. Soc. 2009, 29, 223–236.
15. Sun, H.; Wu, F.; Park, Y.J.; Al Tahtamouni, T.; Li, K.-H.; Alfaraj, N.; Detchprohm, T.; Dupuis, R.D.; Li, X. Influence of TMAl preflow on AlN epitaxy on sapphire. Appl. Phys. Lett. 2017, 110, 192106.
16. Wang, J.; Xu, F.; He, C.; Zhang, L.; Lu, L.; Wang, X.; Qin, Z.; Shen, B. High quality AlN epilayers grown on nitrided sapphire by metal organic chemical vapor deposition. Sci. Rep. 2017, 7, 42747.
17. Miyagawa, R.; Yang, S.; Miyake, H.; Hiramatsu, K.; Kuwahara, T.; Mitsuhara, M.; Kuwano, N. Microstructure of AlN grown on a nucleation layer on a sapphire substrate. Appl. Phys. Express 2012, 5, 25501.

18. Mohn, S.; Stolyarchuk, N.; Markurt, T.; Kirste, R.; Hoffmann, M.P.; Collazo, R.; Courville, A.; Di Felice, R.; Sitar, Z.; Vennéguès, P. Polarity control in group-III nitrides beyond pragmatism. Phys. Rev. Appl. 2016, 5, 54004.
19. Funato, M.; Shibaoka, M.; Kawakami, Y. Heteroepitaxy mechanisms of AlN on nitridated c-and a-plane sapphire substrates. J. Appl. Phys. 2017, 121, 85304.
20. Banal, R.G.; Funato, M.; Kawakami, Y. Initial nucleation of AlN grown directly on sapphire substrates by metal-organic vapor phase epitaxy. Appl. Phys. Lett. 2008, 92, 241905.
21. Shatalov, M.; Sun, W.; Lunev, A.; Hu, X.; Dobrinsky, A.; Bilenko, Y.; Yang, J.; Shur, M.; Gaska, R.; Moe, C. AlGaN deep-ultraviolet light-emitting diodes with external quantum efficiency above 10%. Appl. Phys. Express 2012, 5, 82101.
22. He, C.; Wu, H.; Jia, C.; Zhang, K.; He, L.; Wang, Q.; Li, J.; Liu, N.; Zhang, S.; Zhao, W. Low-Defect-Density Aluminum Nitride (AlN) Thin Films Realized by Zigzag Macrostep-Induced Dislocation Redirection. Cryst. Growth Des. 2021, 21, 3394–3400.
23. Hirayama, H.; Maeda, N.; Fujikawa, S.; Toyoda, S.; Kamata, N. Recent progress and future prospects of AlGaN-based high-efficiency deep-ultraviolet light-emitting diodes. Jpn. J. Appl. Phys. 2014, 53, 100209.
24. Yan, J.; Wang, J.; Zhang, Y.; Cong, P.; Sun, L.; Tian, Y.; Zhao, C.; Li, J. AlGaN-based deep-ultraviolet light-emitting diodes grown on high-quality AlN template using MOVPE. J. Cryst. Growth 2015, 414, 254–257.
25. Imura, M.; Nakano, K.; Kitano, T.; Fujimoto, N.; Narita, G.; Okada, N.; Balakrishnan, K.; Iwaya, M.; Kamiyama, S.; Amano, H. Microstructure of epitaxial lateral overgrown AlN on trench-patterned AlN template by high-temperature metal-organic vapor phase epitaxy. Appl. Phys. Lett. 2006, 89, 221901.
26. Long, H.; Dai, J.; Zhang, Y.; Wang, S.; Tan, B.; Zhang, S.; Xu, L.; Shan, M.; Feng, Z.C.; Kuo, H.-c. High quality 10.6 μ m AlN grown on pyramidal patterned sapphire substrate by MOCVD. Appl. Phys. Lett. 2019, 114, 42101.
27. Zeimer, U.; Kueller, V.; Knauer, A.; Mogilatenko, A.; Weyers, M.; Kneissl, M. High quality AlGaN grown on ELO AlN/sapphire templates. J. Cryst. Growth 2013, 377, 32–36.
28. Dong, P.; Yan, J.; Wang, J.; Zhang, Y.; Geng, C.; Wei, T.; Cong, P.; Zhang, Y.; Zeng, J.; Tian, Y.; et al. 282-nm AlGaN-based deep ultraviolet light-emitting diodes with improved performance on nano-patterned sapphire substrates. Appl. Phys. Lett. 2013, 102, 241113.
29. Conroy, M.; Zubialevich, V.Z.; Li, H.; Petkov, N.; Holmes, J.D.; Parbrook, P.J. Epitaxial lateral overgrowth of AlN on self-assembled patterned nanorods. J. Mater. Chem. C 2015, 3, 431–437.

30. Zhang, L.; Xu, F.; Wang, J.; He, C.; Guo, W.; Wang, M.; Sheng, B.; Lu, L.; Qin, Z.; Wang, X. High-quality AlN epitaxy on nano-patterned sapphire substrates prepared by nano-imprint lithography. Sci. Rep. 2016, 6, 35934.
31. Miyake, H.; Nishio, G.; Suzuki, S.; Hiramatsu, K.; Fukuyama, H.; Kaur, J.; Kuwano, N. Annealing of an AlN buffer layer in N2–CO for growth of a high-quality AlN film on sapphire. Appl. Phys. Express 2016, 9, 25501.
32. Ben, J.; Shi, Z.; Zang, H.; Sun, X.; Liu, X.; Lü, W.; Li, D. The formation mechanism of voids in physical vapor deposited AlN epilayer during high temperature annealing. Appl. Phys. Lett. 2020, 116, 251601.
33. Wang, D.; Uesugi, K.; Xiao, S.; Norimatsu, K.; Miyake, H. Low dislocation density AlN on sapphire prepared by double sputtering and annealing. Appl. Phys. Express 2020, 13, 95501.
34. Susilo, N.; Hagedorn, S.; Jaeger, D.; Miyake, H.; Zeimer, U.; Reich, C.; Neuschulz, B.; Sulmoni, L.; Guttmann, M.; Mehnke, F.; et al. AlGaN-based deep UV LEDs grown on sputtered and high temperature annealed AlN/sapphire. Appl. Phys. Lett. 2018, 112, 41110.
35. Wang, J.; Xu, F.; Liu, B.; Lang, J.; Zhang, N.; Kang, X.; Qin, Z.; Yang, X.; Wang, X.; Ge, W.; et al. Control of dislocations in heteroepitaxial AlN films by extrinsic supersaturated vacancies introduced through thermal desorption of heteroatoms. Appl. Phys. Lett. 2021, 118, 162103.
36. Liu, Z.; Guo, Y.; Yan, J.; Zeng, Y.; Wang, J.; Li, J. Polarity tuning of crystalline AlN films utilizing trace oxygen involved sputtering and post-high-temperature annealing. Appl. Phys. Express 2021, 14, 85501.
37. Chang, H.; Chen, Z.; Li, W.; Yan, J.; Hou, R.; Yang, S.; Liu, Z.; Yuan, G.; Wang, J.; Li, J. Graphene-assisted quasi-van der Waals epitaxy of AlN film for ultraviolet light emitting diodes on nano-patterned sapphire substrate. Appl. Phys. Lett. 2019, 114, 91107.
38. Chang, H.; Liu, B.; Liang, D.; Gao, Y.; Yan, J.; Liu, Z.; Liu, Z.; Wang, J.; Li, J.; Gao, P. Graphene-induced crystal-healing of AlN film by thermal annealing for deep ultraviolet light-emitting diodes. Appl. Phys. Lett. 2020, 117, 181103.
39. Jain, R.; Sun, W.; Yang, J.; Shatalov, M.; Hu, X.; Sattu, A.; Lunev, A.; Deng, J.; Shturm, I.; Bilenko, Y. Migration enhanced lateral epitaxial overgrowth of AlN and AlGaN for high reliability deep ultraviolet light emitting diodes. Appl. Phys. Lett. 2008, 93, 51113.
40. Sun, X.; Li, D.; Chen, Y.; Song, H.; Jiang, H.; Li, Z.; Miao, G.; Zhang, Z. In situ observation of two-step growth of AlN on sapphire using high-temperature metal–organic chemical vapour deposition. CrystEngComm 2013, 15, 6066–6073.
41. Li, X.H.; Wang, S.; Xie, H.; Wei, Y.O.; Kao, T.T.; Satter, M.M.; Shen, S.C.; Douglas Yoder, P.; Detchprohm, T.; Dupuis, R.D. Growth of high-quality AlN layers on sapphire substrates at

relatively low temperatures by metalorganic chemical vapor deposition. Phys. Status Solidi B 2015, 252, 1089–1095.

42. Chen, S.; Li, Y.; Ding, Y.; Li, S.; Zhang, M.; Wu, Z.; Fang, Y.; Dai, J.; Chen, C. Defect reduction in AlN epilayers grown by MOCVD via intermediate-temperature interlayers. J. Electron. Mater. 2015, 44, 217–221.
43. Hagedorn, S.; Knauer, A.; Mogilatenko, A.; Richter, E.; Weyers, M. AlN growth on nano-patterned sapphire: A route for cost efficient pseudo substrates for deep UV LEDs. Phys. Status Solidi A 2016, 213, 3178–3185.
44. Wang, T.Y.; Liang, J.H.; Fu, G.W.; Wuu, D.S. Defect annihilation mechanism of AlN buffer structures with alternating high and low V/III ratios grown by MOCVD. CrystEngComm 2016, 18, 9152–9159.
45. Su, X.; Zhang, J.; Huang, J.; Zhang, J.; Wang, J.; Xu, K. Defect structure of high temperature hydride vapor phase epitaxy-grown epitaxial (0001) AlN/sapphire using growth mode modification process. J. Cryst. Growth 2017, 467, 82–87.
46. Hagedorn, S.; Walde, S.; Mogilatenko, A.; Weyers, M.; Cancellara, L.; Albrecht, M.; Jaeger, D. Stabilization of sputtered AlN/sapphire templates during high temperature annealing. J. Cryst. Growth 2019, 512, 142–146.
47. Chen, Z.; Hoo, J.; Chen, Y.; Wang, V.; Guo, S. Study of AlN based materials grown on nano-patterned sapphire substrates for deep ultraviolet LED applications. Jpn. J. Appl. Phys. 2019, 58, SC1007.
48. Ruschel, J.; Glaab, J.; Susilo, N.; Hagedorn, S.; Walde, S.; Ziffer, E.; Cho, H.K.; Ploch, N.L.; Wernicke, T.; Weyers, M. Reliability of UVC LEDs fabricated on AlN/sapphire templates with different threading dislocation densities. Appl. Phys. Lett. 2020, 117, 241104.
49. Tang, B.; Hu, H.; Wan, H.; Zhao, J.; Gong, L.; Lei, Y.; Zhao, Q.; Zhou, S. Growth of high-quality AlN films on sapphire substrate by introducing voids through growth-mode modification. Appl. Surf. Sci. 2020, 518, 146218.
50. Moram, M.; Vickers, M. X-ray diffraction of III-nitrides. Rep. Prog. Phys. 2009, 72, 36502.
51. Koleske, D.; Figiel, J.; Alliman, D.; Gunning, B.; Kempisty, J.; Creighton, J.; Mishima, A.; Ikenaga, K. Metalorganic vapor phase epitaxy of AlN on sapphire with low etch pit density. Appl. Phys. Lett. 2017, 110, 232102.